4D MRI-Based Stability Assessment of Carpal Kinematic Metrics

Azadeh Sharafi[1] , Andrew S. Nencka[1], and Kevin M Koch [1]
[1]Medical College of Wisconsin, Milwaukee, WI
asharafi@mcw.edu

Disclosures: The Authors have nothing to disclose.

INTRODUCTION:

Carpal instability severely impacts daily life, causing discomfort and hampering regular tasks. While traditional diagnostic methods depend on static imaging, they overlook the dynamic nature of carpal bone movements. There's a growing interest in dynamic imaging, such as CT or MRI, which seek to capture real-time wrist movements. MRI, in particular, offers non-invasive and comprehensive assessments without ionizing radiation risks. This study builds on our previous work [1], aiming to create metrics for wrist motion analysis and assess stability across different cohorts with and without past wrist injuries.

METHODS:

20 participants with- and 29 without a history of wrist injury provided written consent to participate in an IRB-approved study. Participants underwent imaging using a 3T MRI scanner, positioned supine for static and prone for dynamic scans, with the wrist being studied centered within the center of the coils. Strategic placement of positioning pads ensured stability and the necessary freedom for movement during dynamic imaging. Static imaging was achieved using a commercial 3D 2-point Dixon sequence with a voxel size of 0.9mm×0.9mm×1mm. For dynamic imaging, participants executed radial-ulnar deviation and flexion-extension motions three times, following visual cues. 40 3D volumes with a voxel size of 1.6mm×1.6mm×2.5mm across 12 slices were acquired at intervals of 2.6 seconds (Fig.1). Obtaining the water Dixon (i.e., fat-suppressed) images is crucial for automated carpal segmentation needed for bone tracking. Automatic segmentation of scaphoid, lunate, and capitate in the images leveraged a deep convolutional neural network (SegResNet). Utilizing the Iterative Closest Point (ICP) algorithm to register each wrist carpal bone from dynamic frames to its respective position in the static frame. The 4×4 transformation matrices for each carpal bone in the remaining frames were broken down into a 3×1 translation and a 3×3 rotation matrix, subsequently converted into three x-y-x Euler angles. This method efficiently captured the carpal bone movement as rotations and translations along the three axes of the RCS [2] and anchored the kinematics to a neutral wrist position [1]. An algorithm was developed to automatically separate the three motion cycles within subjects [3]. By plotting the scaphoid and lunate motion against the capitate, we provided a straightforward mechanism for self-referenced analysis [1]. We conducted separate linear and quadratic fits for each motion segment to extract distinct kinematic metrics, which yielded 120 carpal kinematic metrics across the two captured motions. The stability of kinematic metrics from participants with and without prior wrist injuries was evaluated. The Intraclass Correlation Coefficient (ICC) was employed to gauge stability both within individuals and across the two groups.

RESULTS:

Fig. 2 illustrates representative plots of the Scaphoid angle versus the capitate angle around three RCS axes, accompanied by their first and second-order polynomial fits. Intra-subject ICC identified 17 of the 120 computed metrics with high levels of stability (ICC > 0.7). Calculated intra-subject ICC values revealed different distribution trends between the two cohorts. The relevant metric stability within the cohorts is best captured by comparing each cohort's 80th and 90th percentile values of the metric ICC distributions. The 90th percentile values stand at 0.76 for the group without a history of injury (asymptomatic), while it was 0.68 in the group with prior injury (symptomatic). Similarly, the 80th percentile values showed more stability within the asymptomatic vs. symptomatic group, with ICC levels of 0.61 and 0.57, respectively.

DISCUSSION:

Our results indicate a greater variance of the most stable MRI-based carpal dynamic metrics within the symptomatic group. Such an observation aligns with the anticipated results and provides encouraging evidence that the derived kinematic metrics hold promises as indicators of carpal dysfunction.

SIGNIFICANCE/CLINICAL RELEVANCE:

This study's results highlight the emerging capability of dynamic MRI to evaluate and delineate intricate carpal bone movements, quantitatively. The stability assessments of the kinematic metrics reveal promising distinctions between groups with and without prior wrist injuries. While these pronounced variations in metric stability underscore the potential value of this method in analyzing carpal instability, additional research is essential to further refine these findings.

REFERENCES:

1. M. Zarenia, V. E. Arpinar, A. S. Nencka, L. T. Muftuler, and K. M. Koch. Dynamic tracking of scaphoid, lunate, and capitate carpal bones using four-dimensional mri. Plos one, 17(6):e0269336, 2022.
2. G. Wu, F. C. Van der Helm, H. D. Veeger, M. Makhsous, P. Van Roy, C. Anglin, J. Nagels, A. R. Karduna, K. McQuade, X. Wang, et al. Isb recommendation on definitions of joint coordinate systems of various joints for the reporting of human joint motion—part ii: shoulder, elbow, wrist and hand. Journal of biomechanics, 38(5):981–992, 2005.
3. Sharafi, A. S. Nencka, and K. M. Koch. Development and stability analysis of carpal kinematic metrics from 4d magnetic resonance imaging. arXiv preprint arXiv:2305.16423, 2023.

ACKNOWLEDGEMENTS:

Research reported in this publication was supported by NIH grant R21AR075327.

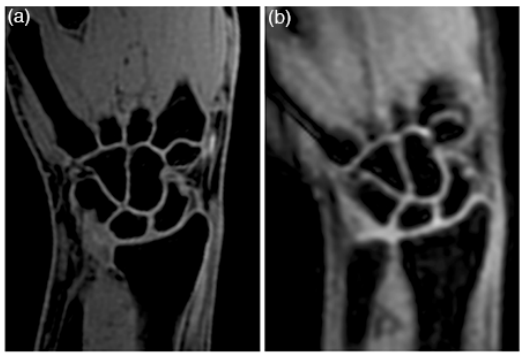

Fig 1. Coronal fat-suppressed slice obtained using a 3D 2-point Dixon sequence. (a) Static wrist image. (b) A snapshot from the dynamic acquisition during radial-ulnar deviation.

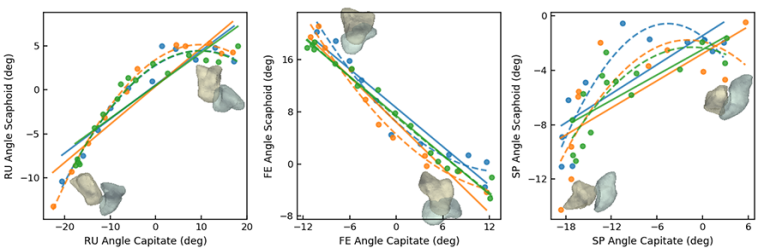

Fig2. Illustrative depiction of the scaphoid's angular deviation in relation to the capitate along RCS axes during radial-ulnar deviation movement. Polynomial fits of the first (solid line) and second (dotted line) degree are showcased for each of the three distinct motion segments, each differentiated by color. The 3D orientations of the scaphoid (in light blue) and capitate (in ivory) at their maximum angular placements are represented by the background meshes.